



May 23, 2014

Oxy-combustion Environmental Characterization: Fire- and Steam-side Corrosion

Gordon R. Holcomb, NETL

Joseph Tylczak, NETL

Bret H. Howard, NETL

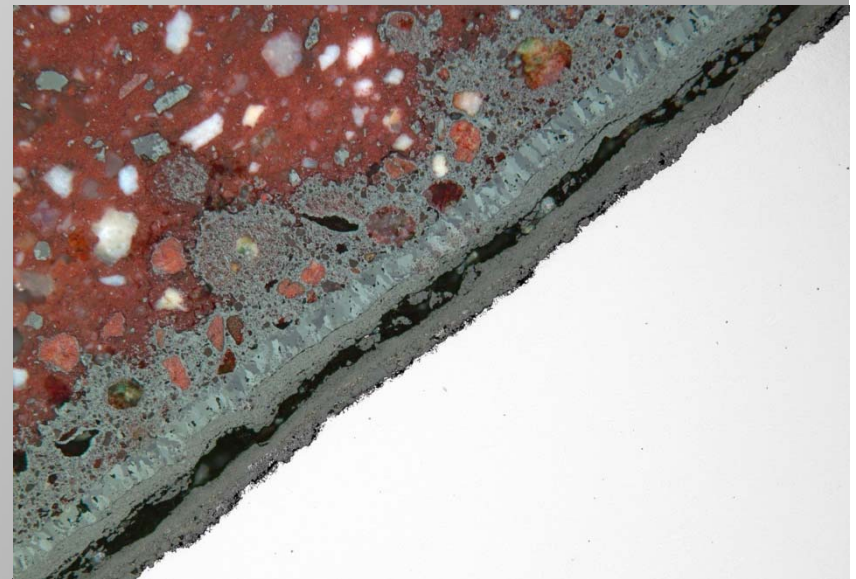
Casey Carney, URS, NETL

Adam Wise, CMU

David E. Laughlin, CMU

N. Meltem Yanar, UPitt

Gerald H. Meier, UPitt



the ENERGY lab

Acknowledgements

- Funding from the Strategic Center for Coal, Cross-Cutting Research
- Susan Maley, NETL, SCC, Technology Manager, Cross-Cutting Research
- Charles Miller, NETL, SCC, Technical Project Monitor, Cross-Cutting Research
- Vito Cedro, NETL, SCC, Project Manager, Cross-Cutting Research
- David Alman, NETL, ORD, Structural Materials Development Division Director
- Jeffrey Hawk, NETL, ORD, Technical Coordinator, ORD's Advanced Combustion FWP

Disclaimer

- "This report was prepared as an account of work sponsored by an agency of the United States Government. Neither the United States Government nor any agency thereof, nor any of their employees, makes any warranty, express or implied, or assumes any legal liability or responsibility for the accuracy, completeness, or usefulness of any information, apparatus, product, or process disclosed, or represents that its use would not infringe privately owned rights. Reference herein to any specific commercial product, process, or service by trade name, trademark, manufacturer, or otherwise does not necessarily constitute or imply its endorsement, recommendation, or favoring by the United States Government or any agency thereof. The views and opinions of authors expressed herein do not necessarily state or reflect those of the United States Government or any agency thereof."

Outline

Fireside Corrosion in Oxy-Fuel Combustion

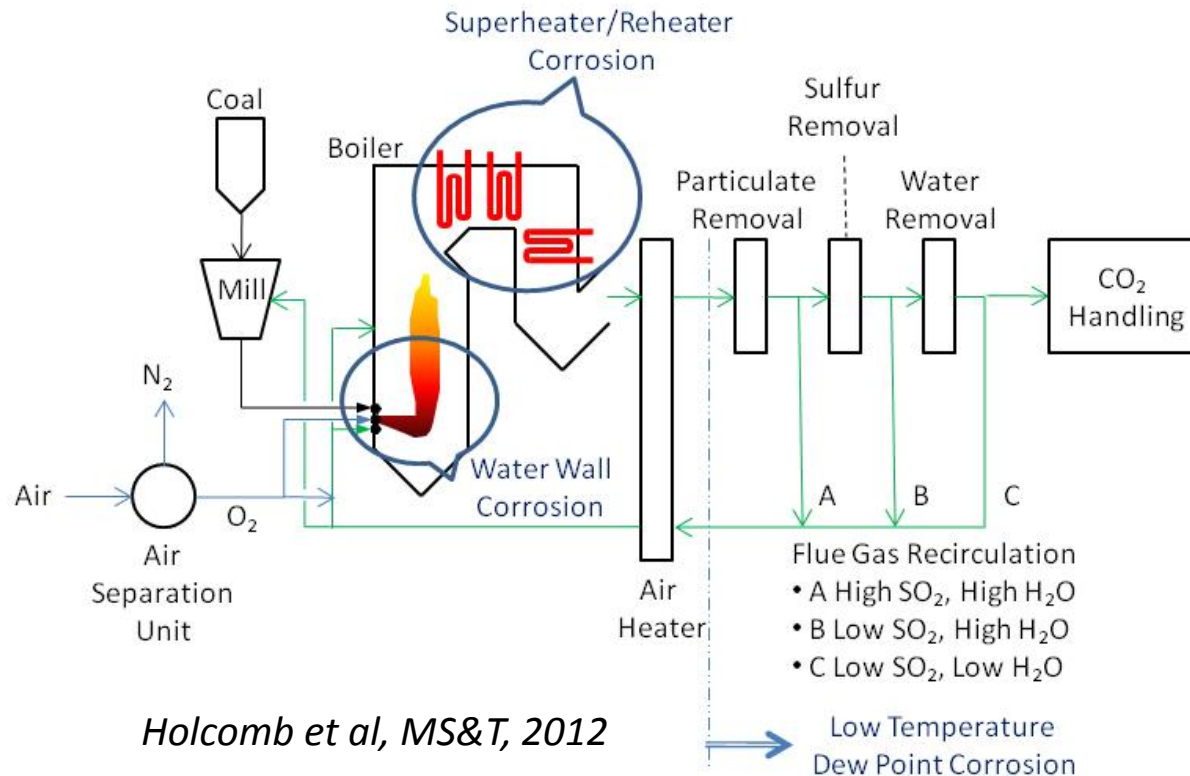
- Brief Background
- Experimental Procedures
- Results
- Conclusions
- New FY14 Research Efforts
- Initial Results

Hydrogen Tracking During Oxidation

- Background
- Experimental Procedures
- Results

Brief Update of Steam Oxidation in A-USC Conditions

Fireside Corrosion Associated with Oxy-Combustion



- CO_2 replaces N_2 as the primary flue gas
- This changes the heat balance in the boiler
- Flue gas recirculation mimics air-fired heat balance

A primary goal was to examine the corrosion effects from flue gas composition changes arising from oxy-combustion

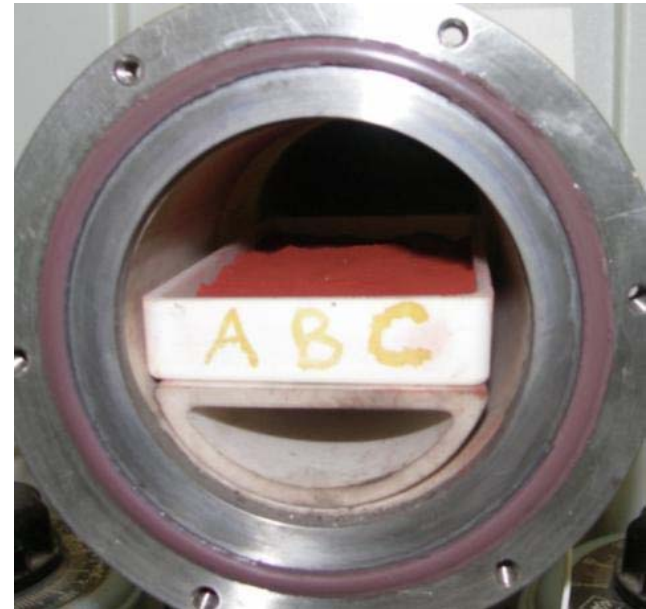
Laboratory Fireside Corrosion—Gas Phase FY12-13

Conditions		700°C, SH/RH Conditions			
		Air-Fired	Oxy-Fired		
			FGD <H ₂ O	FGD	wo FGD
Input Gas	N ₂	Bal	8	8	8
	CO ₂	14	Bal	Bal	Bal
	H ₂ O	9	9	20	20
	O ₂	2.5	2.5	2.5	2.5
	SO ₂	0.3	0.3	0.3	0.9
Calc SO _x	SO ₂	0.215	0.215	0.215	0.649
	SO ₃	0.085	0.085	0.085	0.252

Kung (2010) showed that a SO₂+SO₃ level of 0.3 results from a coal with a sulfur content of 4.3, such as a high sulfur Gatling (OH) bituminous coal

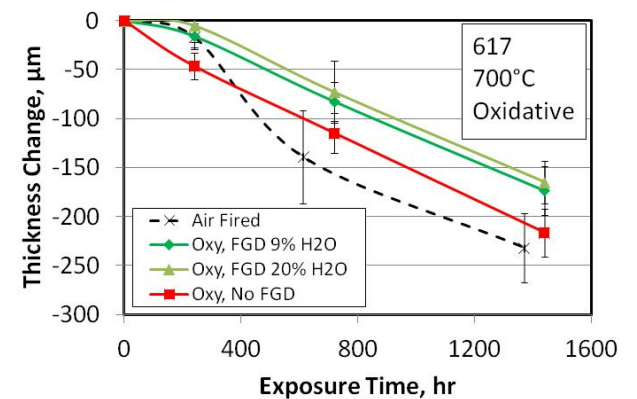
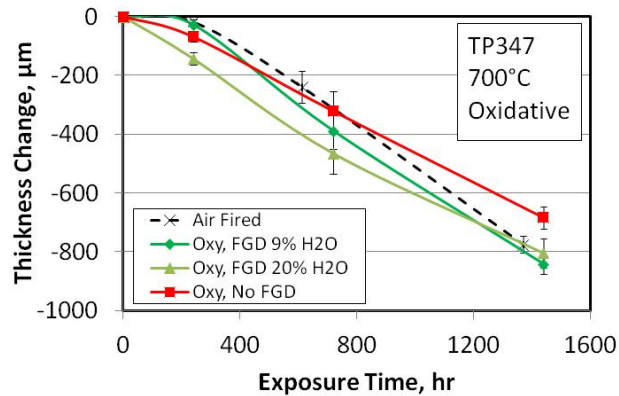
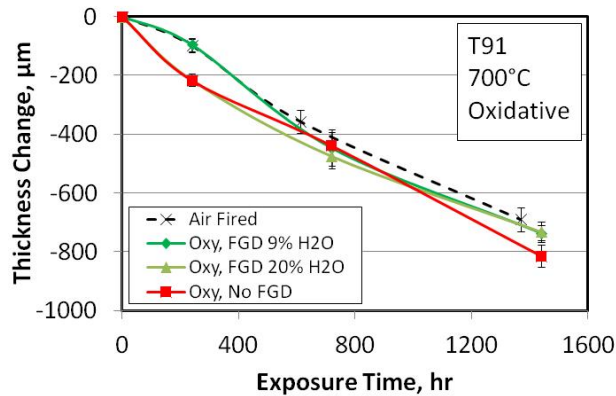
Long-term Laboratory Fireside Corrosion Tests, FY12-13

- **Ash Composition**
30 Fe₂O₃ 30 Al₂O₃ 30 SiO₂ 5 Na₂SO₄ 5 K₂SO₄
- **Ash Application**
 - One side coverage, 3mm thick, 40 g/cm² compaction
- **Triplicate samples**
- **240 hour test segments**
Clean samples of ash after each segment
Weigh, photograph, reapply ash, and test again
- **Special Ash-Retained Samples after 240hr of Exposure**
- **One of the triplicates available for periodic removal of 2 mm of sample for section-loss analysis**
- **25 cm/min gas phase velocity (at temperature)**
- **Pt catalyst for SO₂-O₂-SO₃ equilibrium**
 - Used to keep laboratory gas environment constant and reproducible



Alloy	Fe	Cr	Ni	Co	Mo	C	Si	Ti	Al	Mn	V	Nb+Ta	Cu	Other
T91	Bal	8.46	0.14		0.95	0.10	0.36		0.01	0.44	0.22	0.08	0.16	0.05 N
TP347H	Bal	17.55	11.04	0.10	0.39	0.08	0.57	0.01	0.02	1.57	0.07	0.95	0.35	0.04 W
IN617	0.39	21.87	Bal	11.46	9.65	0.10	0.01	0.47	0.98	0.04		0.03	0.01	

SH/RH Temperatures (700°C)



- Linear corrosion rates
- No significant differences in section loss measurements between air- and oxy-firing at 700°C
- Early trends disappeared with longer exposure times

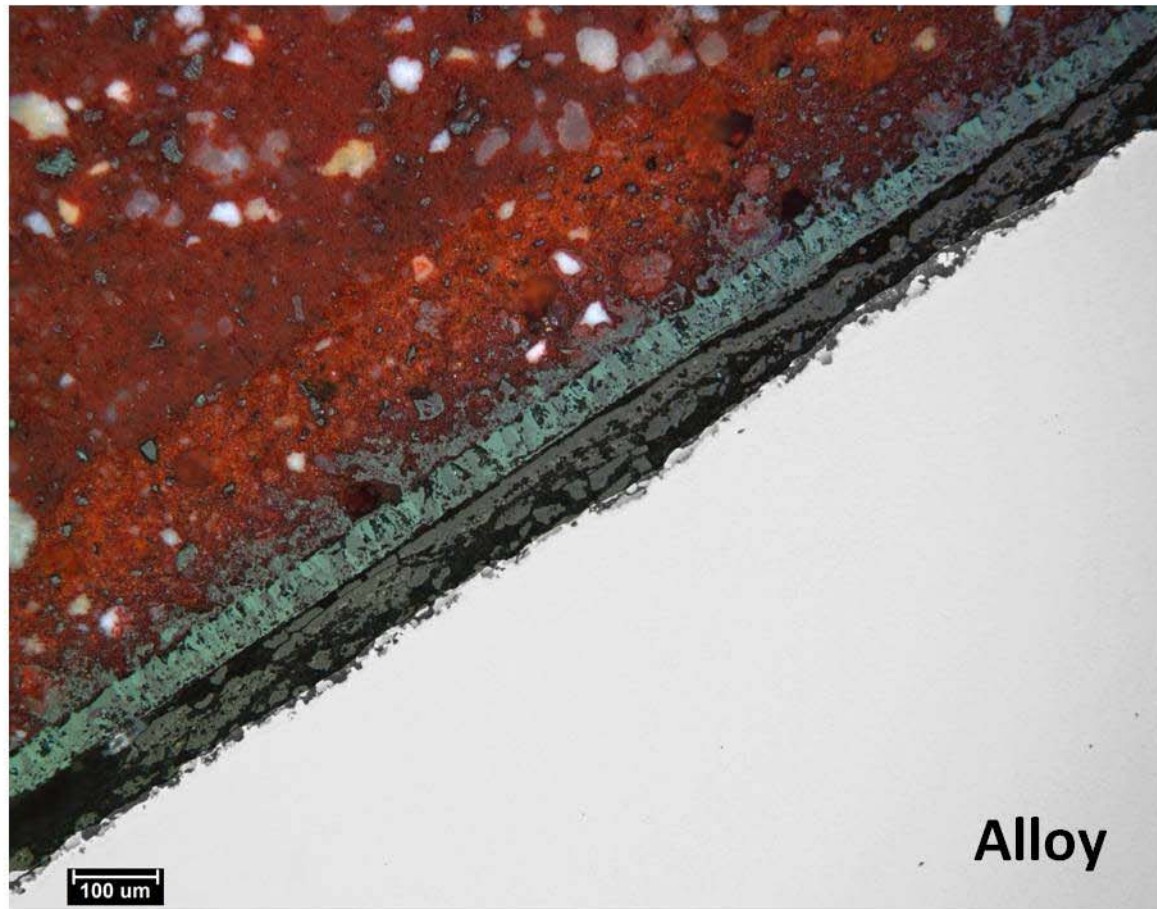
Conditions		700°C, SH/RH Conditions			
		Air-Fired	Oxy-Fired		
			FGD <H ₂ O	FGD	no FGD
Input Gas	N ₂	Bal	8	8	8
	CO ₂	14	Bal	Bal	Bal
	H ₂ O	9	9	20	20
	O ₂	2.5	2.5	2.5	2.5
	SO ₂	0.3	0.3	0.3	0.9

T91 (Oxy FGD 20% H₂O) 240hr at 700°C
CO₂+8%N₂+20%H₂O+2.5%O₂+0.3%SO₂

Special test
with ash
retained

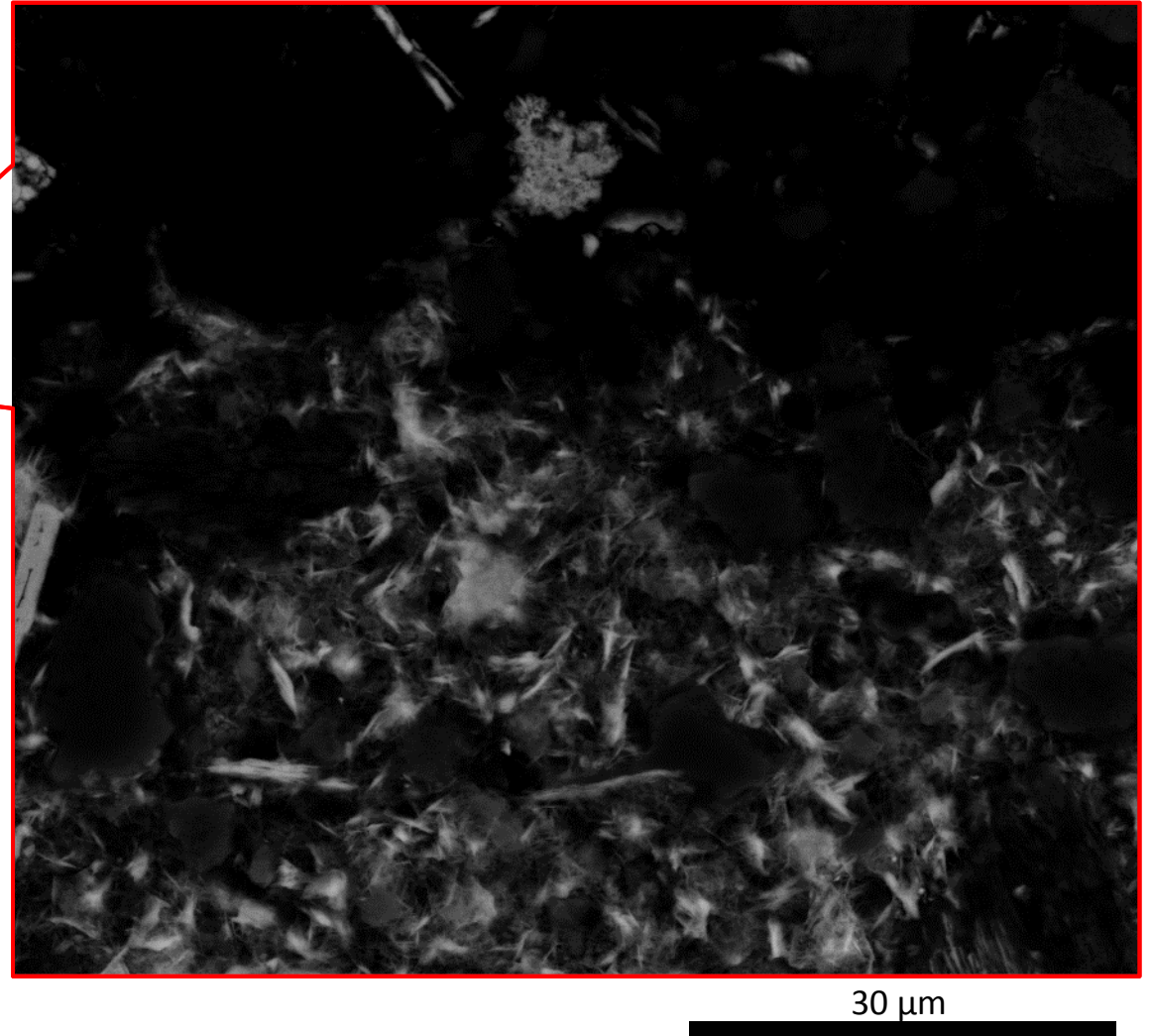
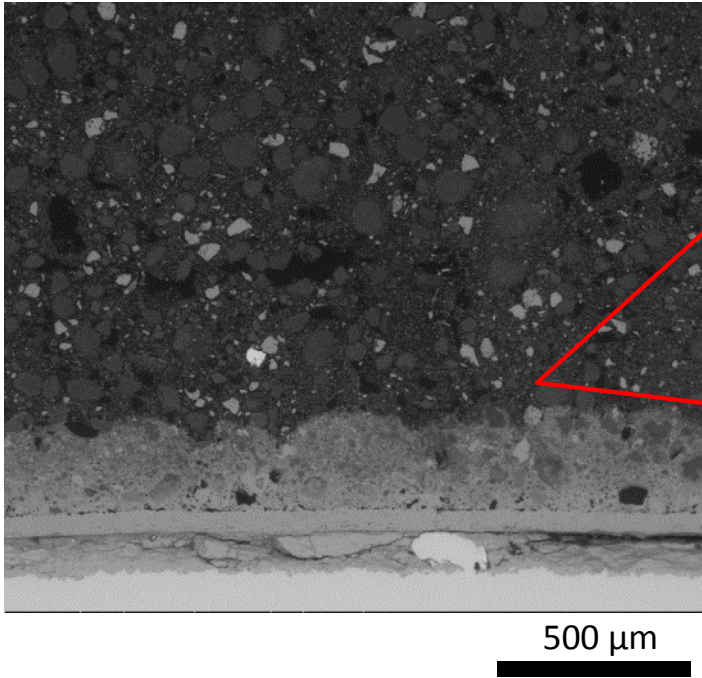
Ash

Ash Affected Zone
Oxide Deposition
Outer Oxide Scale
Inner Oxide Scale



Alloy

T91, Oxy-fired, $\text{CO}_2+8\%\text{N}_2+20\%\text{H}_2\text{O}+2.5\%\text{O}_2+0.3\%\text{SO}_2$, 700°C, 240h

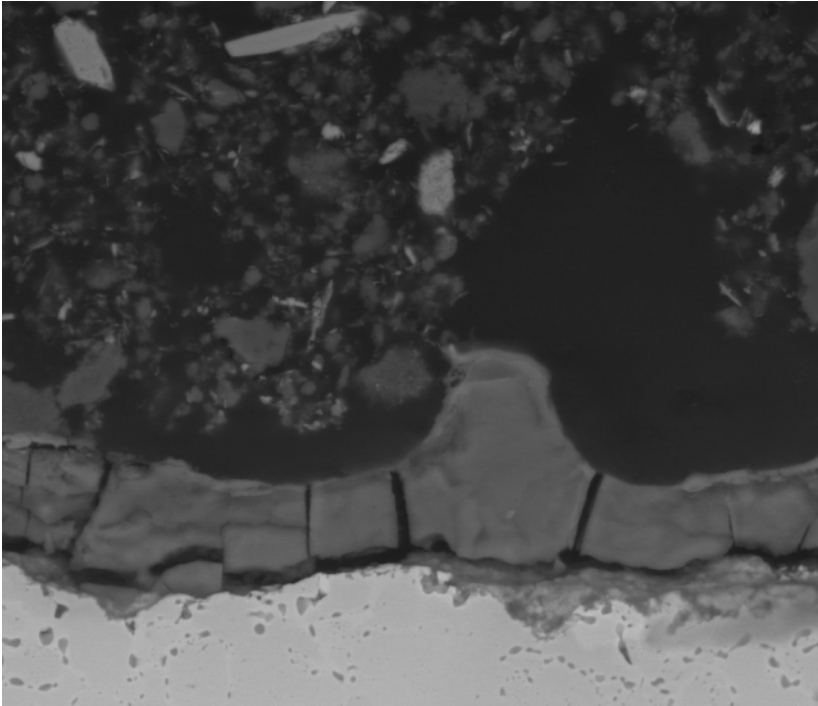


Needle shaped Fe-rich oxides through the pores between the ash particles

617, 240hr at 700°C

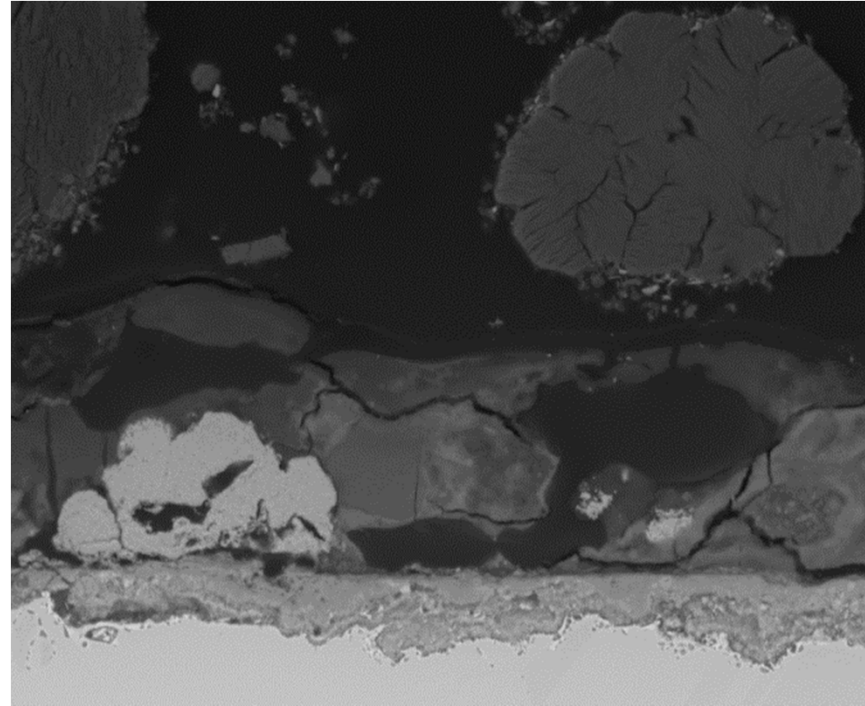
(Oxy FGD 20% H₂O)

CO₂+8%N₂+20%H₂O+2.5%O₂+0.3%SO₂



(Oxy no FGD)

CO₂+8%N₂+20%H₂O+2.5%O₂+0.9%SO₂



50 μm

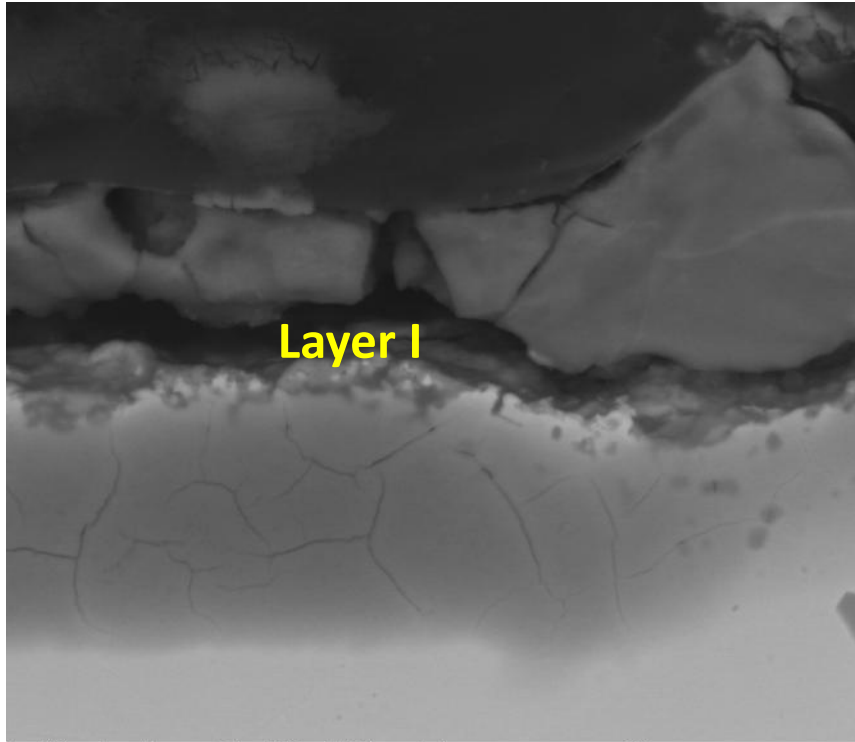
- External scale fused with ash
- More discrete internal sulfide particles beneath the inner scale layer

- External scale fused with ash
- Thicker external scale
- Large NiO particles present
- Large pores present
- Thicker inner S-rich layer

617, 240hr at 700°C

(Oxy FGD 20% H₂O)

CO₂+8%N₂+20%H₂O+2.5%O₂+0.3%SO₂

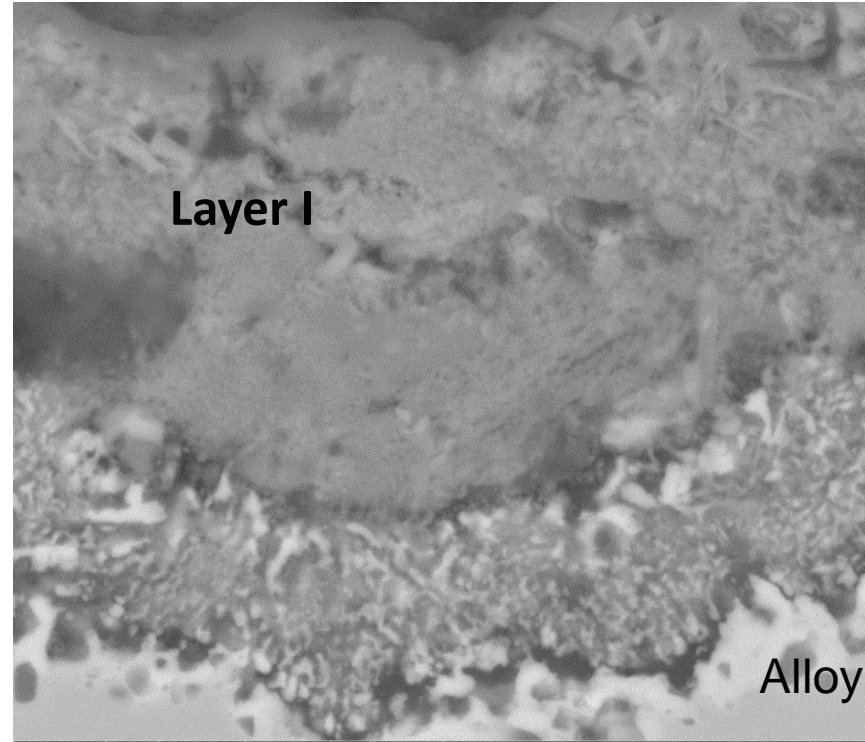


20 µm

- Much thinner layer I
- Intergranular internal sulfides

(Oxy no FGD)

CO₂+8%N₂+20%H₂O+2.5%O₂+0.9%SO₂

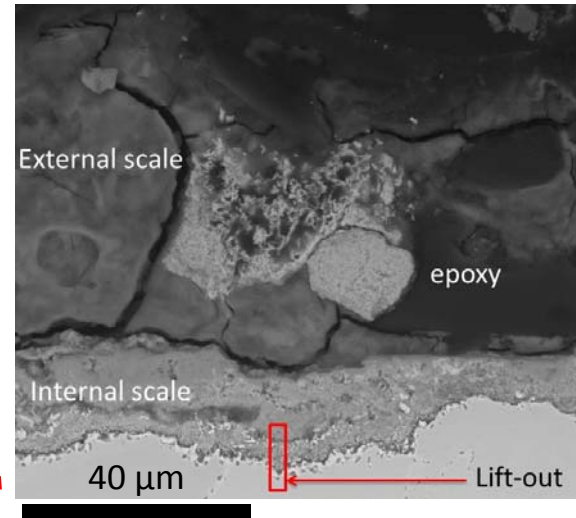
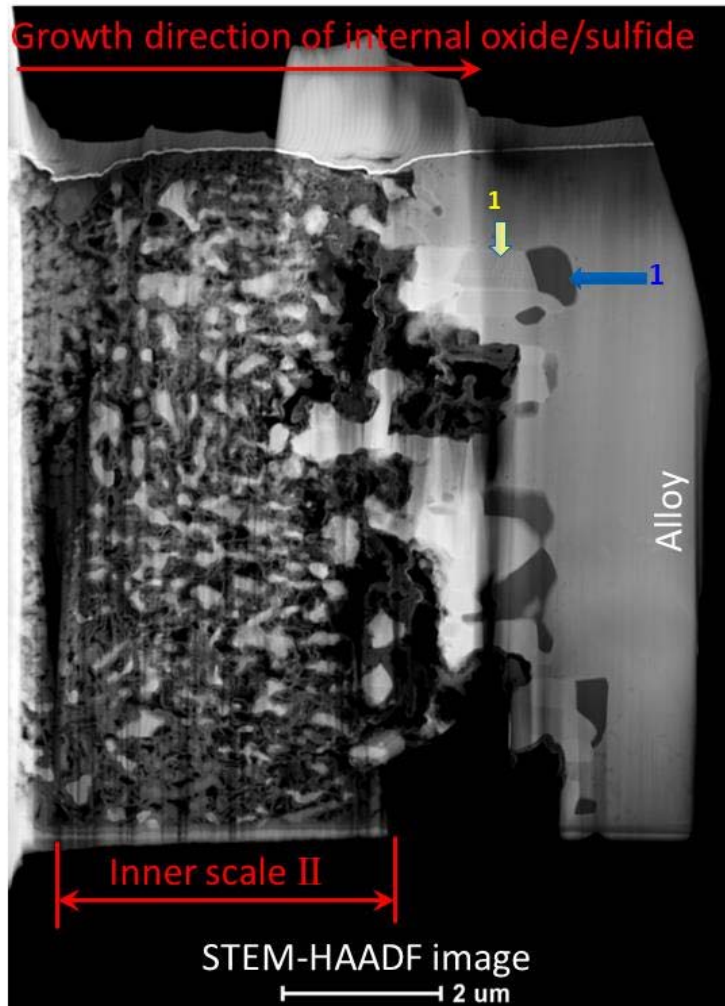


5 µm

- Internal sulfidation morphology

Transmission Electron Microscopy (TEM) Analyses

IN617 oxy-fired: $\text{CO}_2 + 8\% \text{N}_2 + 20\% \text{H}_2\text{O} + 2.5\% \text{O}_2 + 0.9\% \text{SO}_2$ 700°C & 240 hr



at %	1	1
O(K)	5.86	25.73
S(K)	11.66	33.40
Cr(K)	0.13	40.74
Fe(K)	0.37	0.03
Co(K)	15.54	0.01
Ni(K)	44.35	0.05
Mo(K)	22.06	0

- Internal oxidation, sulfidation of Cr (blue).
- Alloy above internal sulfides are low in Cr (yellow).
- Rapid corrosion.

Conclusions: 700°C Oxy-combustion Corrosion

Overall

- Corrosion rates at 700°C did not change with flue gas composition (ash chemistry held constant)
- Substantial metal loss, linear with time

T91

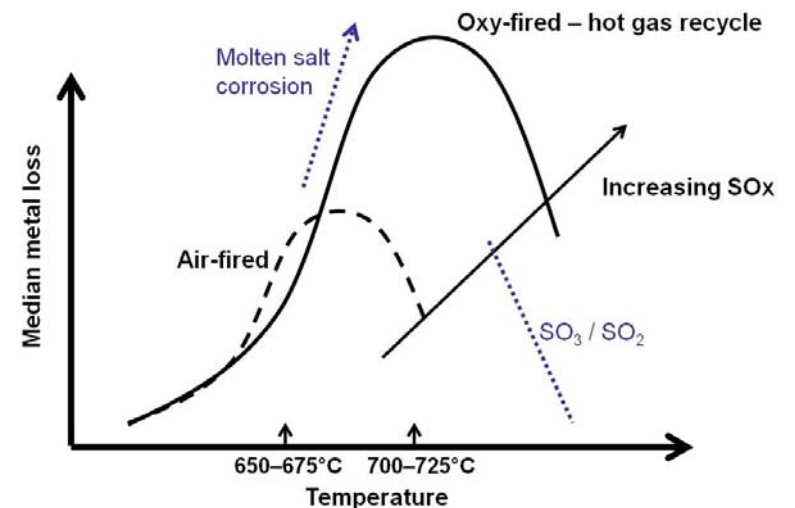
- Ash attachment, needle-shaped iron oxide growing into and infiltrating the ash

617

- Morphology change at high SO₂—more internal sulfidation of Cr
- Internal sulfidation leads to low Cr levels in the alloy between the internal sulfide and scale, which may lead to increased corrosion at longer times

New FY 14 Research Effort

- **Focus is on these items**
 - Examine reports of a shift upwards in the temperature of maximum corrosion for oxy-combustion conditions. Implications for A-USC steam boilers.
 - Use model alloys to examine the effect of Mo in Ni-Cr alloys. Several A-USC Ni-base alloys of interest contain up to 8-10% Mo.
 - Compare NETL's CPJ7B to T92
 - Look at sulfate flux as a variable in the ash as a tool to address oxy-combustion ash changes
- **Ni-base alloys**
 - Model alloys Ni-22Cr, Ni-22Cr-1Mo and Ni-22Cr-8Mo
 - Commercial A-USC alloy 740H
- **9Cr Ferritic/Martensitic Steels**
 - T92 and CPJ7B
- **Gas Compositions**
 - Air-firing: $N_2-14CO_2-9H_2O-2.5O_2-0.3SO_2$
 - Oxy-firing: $CO_2-8N_2-20H_2O-2.5O_2-0.9SO_2$ (hot gas recycle case)
- **Temperatures**
 - 650, 675, 700, 725, 750, 775, 800°C



N. Simms, T. Hussain and A. Syed (2012.)

Additional Test Details

- **Ash Composition (see table)**
 - Maintain 3:1 ratio of $(\text{Na,K})_2\text{SO}_4:\text{Fe}_2\text{O}_3$ as found in lowest melting point alkali iron trisulfates
 - S20 closest to prior ash composition (30 Al_2O_3 30 SiO_2 30 Fe_2O_3 5 Na_2SO_4 5 K_2SO_4)
- **Special Ash-Retained Samples after 24hr of Exposure**

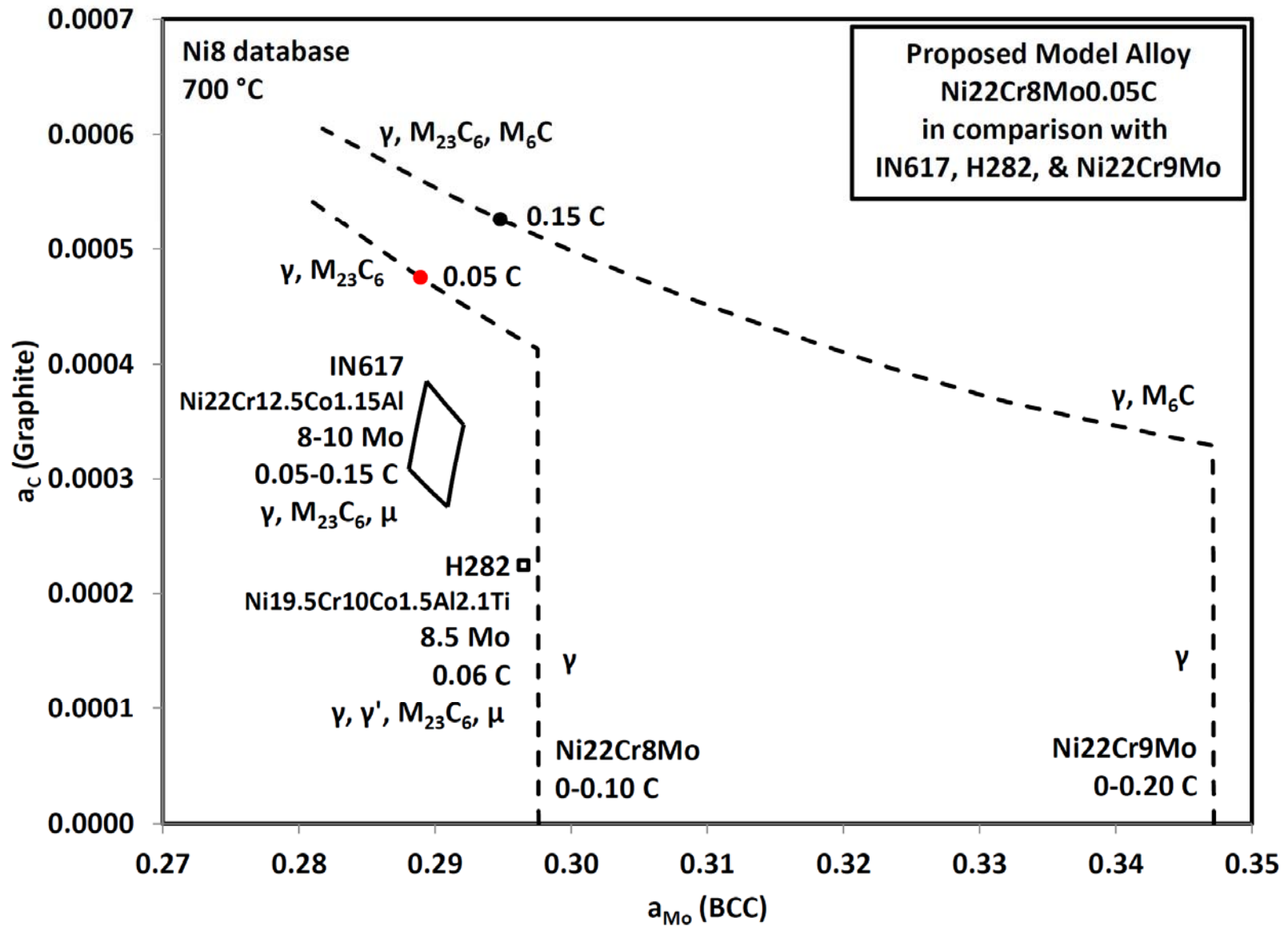
ID	Al_2O_3	SiO_2	Fe_2O_3	Na_2SO_4	K_2SO_4
SCM	0	0	25	37.5	37.5
S80	10	10	20	30	30
S60	20	20	15	22.5	22.5
S40	30	30	10	15	15
S20	40	40	5	7.5	7.5

Effect of Mo in Ni-Cr Alloys

- **Hot Corrosion Research, focused primarily on turbine applications, reports severe degradation with Mo in Ni-base superalloys**
 - MoO_2 reacted with Na_2SO_4 to produce an acid (SO_2 -rich) salt, leading to acidic fluxing, Pettit and Meier (1985)
 - MoO_3 incorporated into Na_2SO_4 by the formation of compounds such as Na_2MoO_4 , $\text{Na}_2\text{MoO}_4 \cdot \text{MoO}_3$, and $\text{Na}_2\text{MoO}_4 \cdot 2\text{MoO}_4$ can be liquid and have a high solubility for Cr_2O_3 , Fyrburg et al (1982)
 - A reported threshold for Mo below which catastrophic attack is not encountered. For Ni-15% Cr at 900°C the threshold was between 3-4% Mo, Peters et al (1976)
- **Mo is significant in many Ni-base A-USC superalloys:**

<u>Significant Mo</u>	<u>Modest Mo</u>
263: Ni 20.0Cr 6.0Mo	230: 22.0Cr 2.0Mo
282: Ni 19.5Cr 8.5Mo	740: 25.0Cr 0.5Mo
617: Ni 22.0Cr 9.0Mo	
625: Ni 21.5Cr 9.0Mo	
- **Model Ni-22Cr-XMo alloys will be used to assess corrosion initiation and propagation as a function of Mo. 15 lb heats of each were made by Paul Jablonski.**

Ni-22Cr-8Mo-0.05C Model Alloy



Alloys Tested—Alloys Compositions (wt%)

FY14

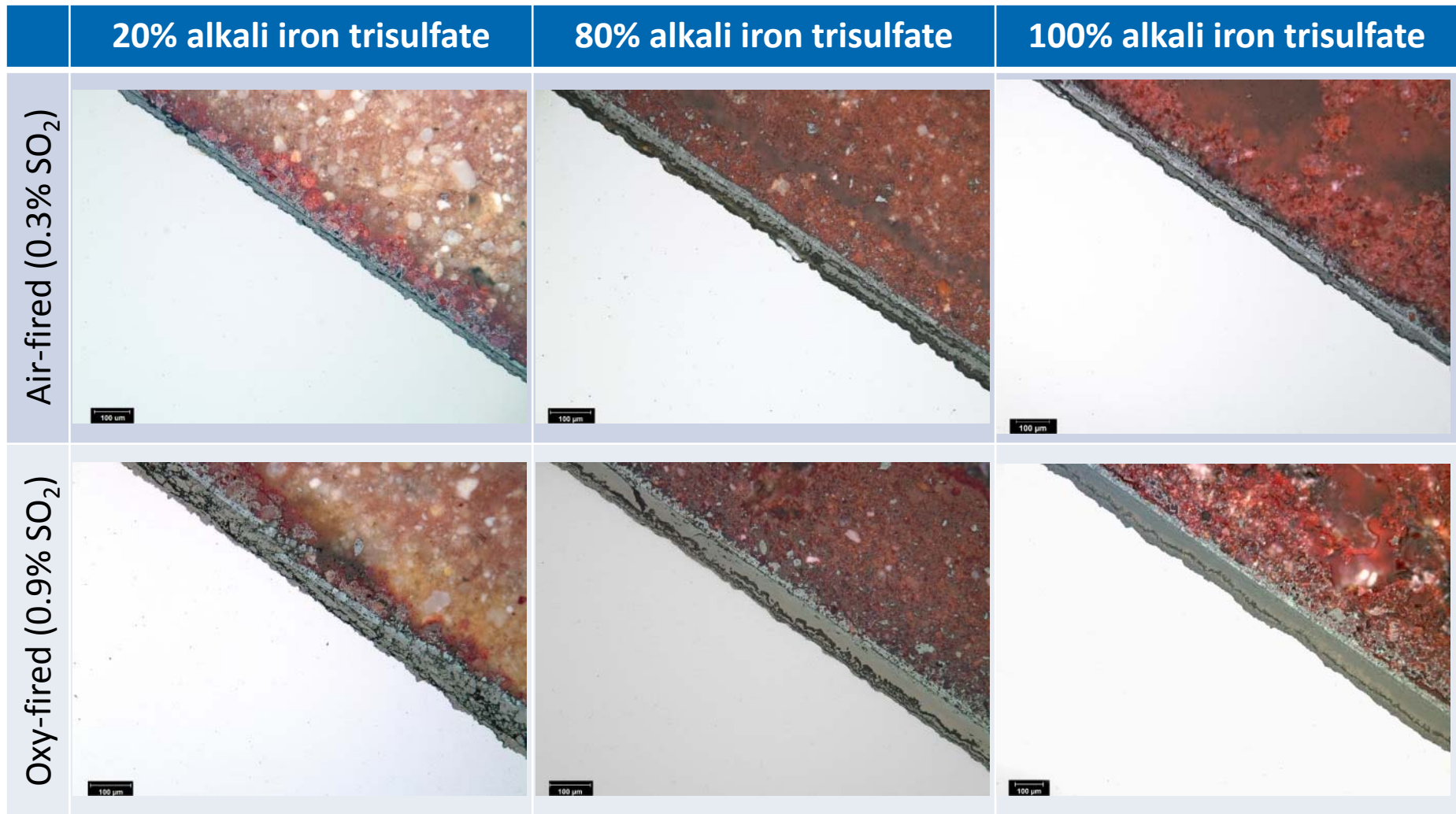
Alloy	Fe	Cr	Ni	Co	Mo	C	Si	Ti	Al	Mn	V	Nb+Ta	Cu	Other
T92	Bal	9.08	0.25	0.01	0.45	0.081	0.09		0.01	0.40	0.21	0.07		1.80 W
CPJ7B In Dev	Bal	9												
740H Nominal	0.7	25	Bal	20	0.5		0.15	1.35	1.35	0.3		1.5		
Ni22Cr 0Mo		22.18	Bal		0.02	0.043		0.01	0.08			0.01	0.01	11 ppm S
Ni22Cr 1Mo		22.04	Bal		0.99	0.050			0.07			0.02	0.01	4 ppm S
Ni22Cr 8Mo		22.04	Bal		7.77	0.052			0.07			0.01		11 ppm S

Met target Cr, Mo, and C levels in Ni-22Cr-xMo model alloys
Low S levels obtained

Preliminary Results

- **Light microscopy images from ash-retained 24hr tests**
 - Iron oxide fluxing evident in T92
 - Effect of Mo on corrosion initiation

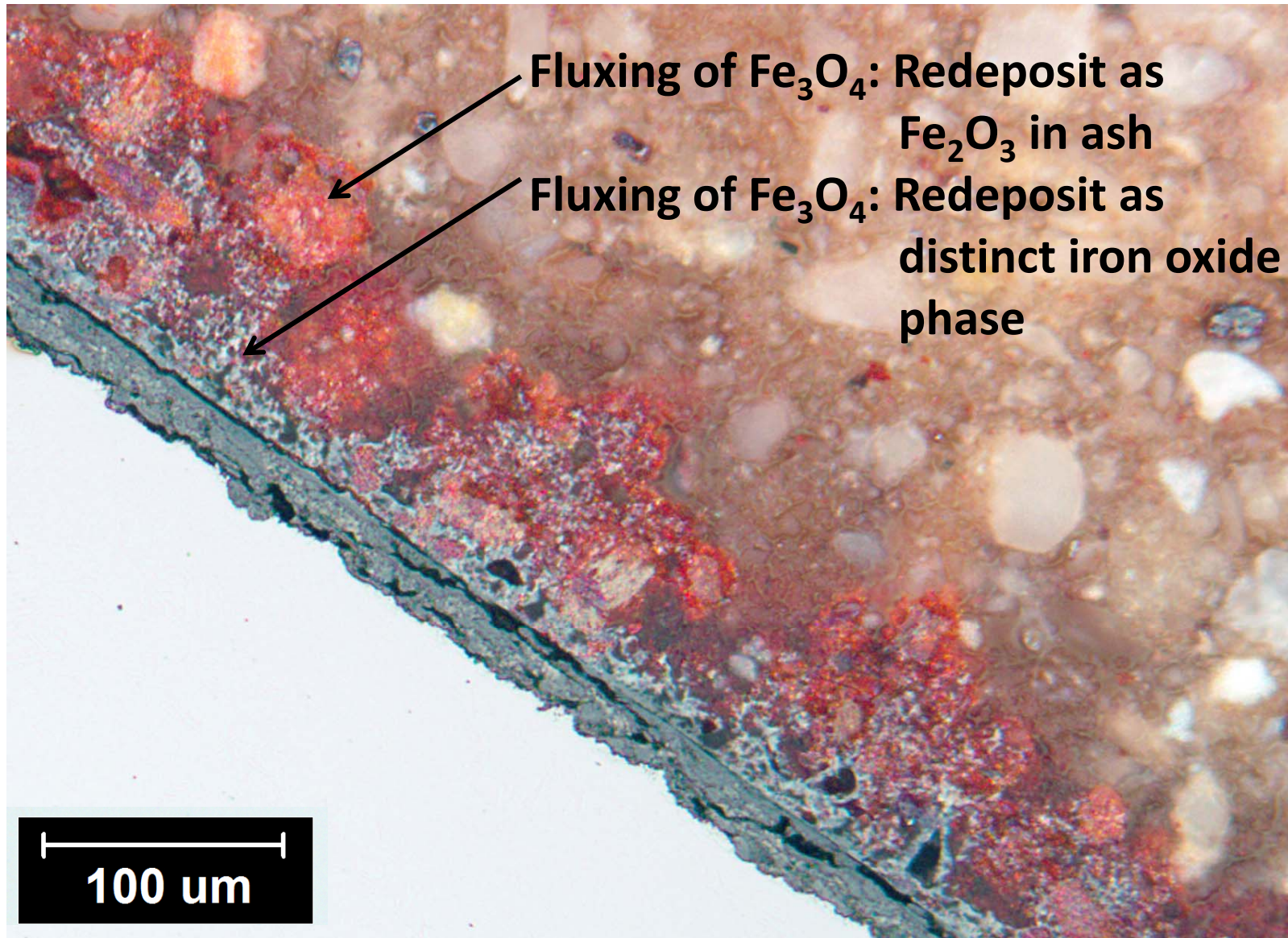
24 hr Ash-Retained Tests – T92 at 700°C



Little effect from Ash Content on Scale Thickness

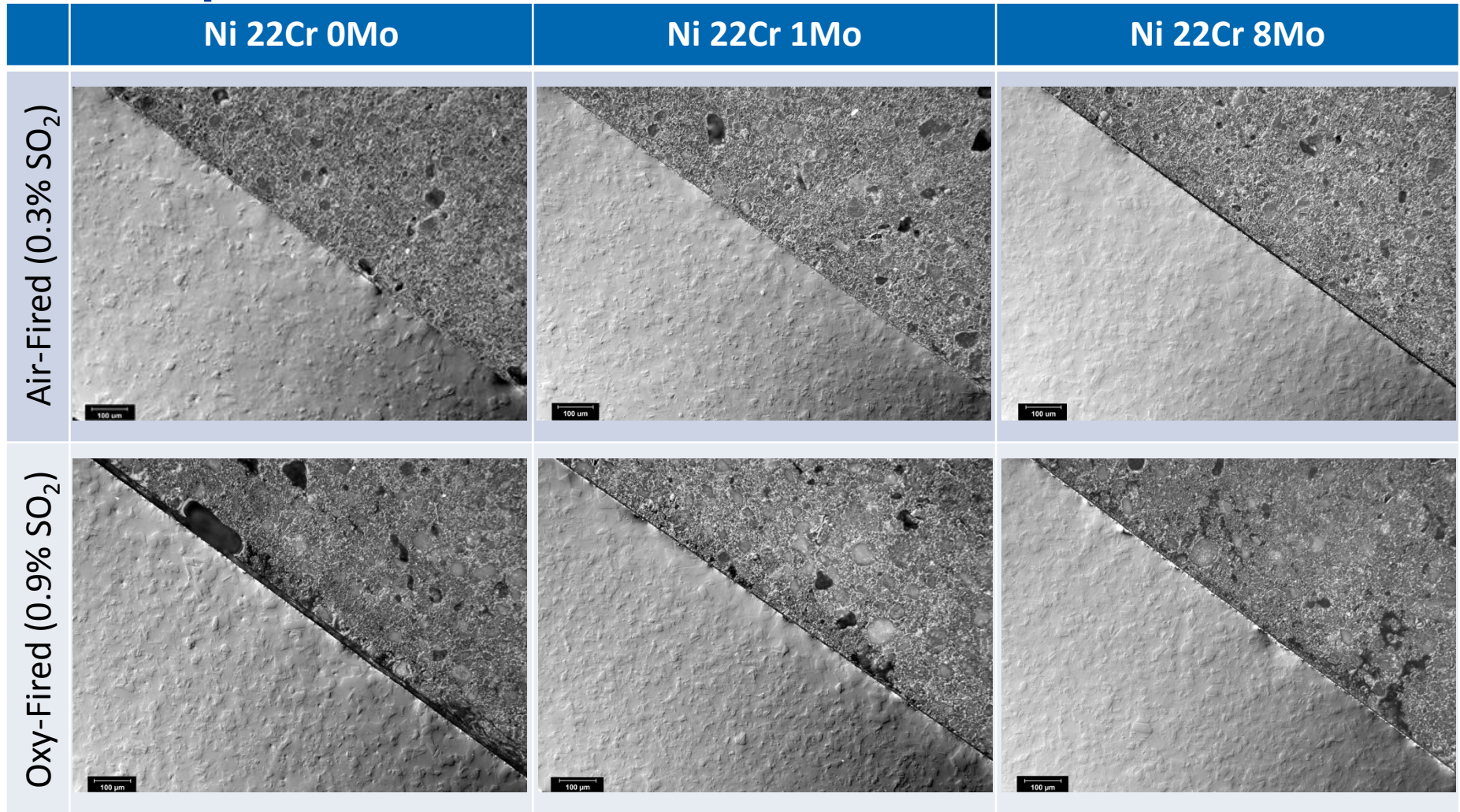
Some effect from Gas Phase (SO_x, H₂O, CO₂) on Scale Thickness

24 hr Air-Fired Exposure of T92 at 700°C with a 20% alkali iron trisulfate ash



Effect of Mo

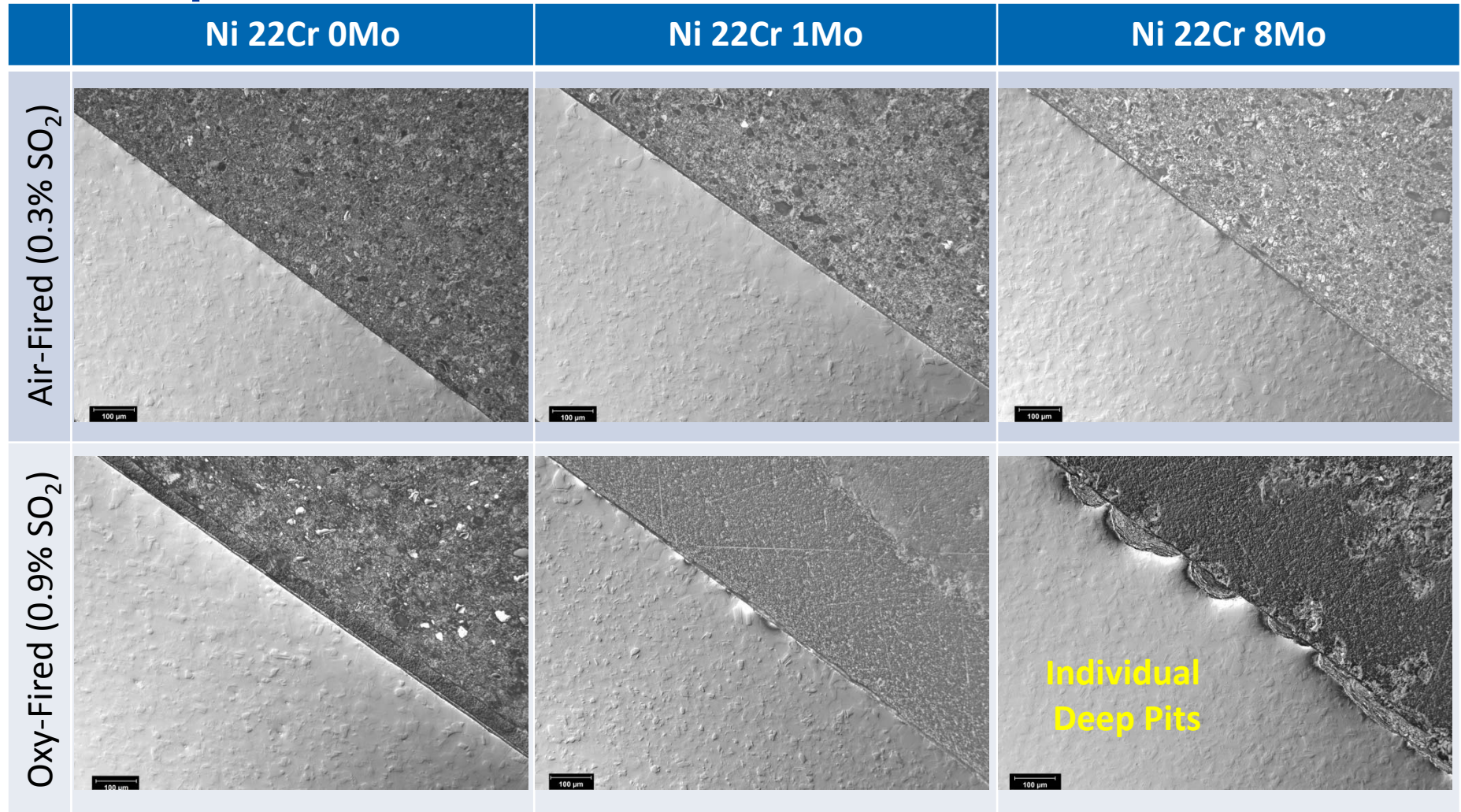
24 hr Exposure at 700°C with a **20%** alkali iron trisulfate ash



No effect from Mo or Gas Phase (SO_x, H₂O, CO₂) with a 20% alkali iron trisulfate ash

Effect of Mo

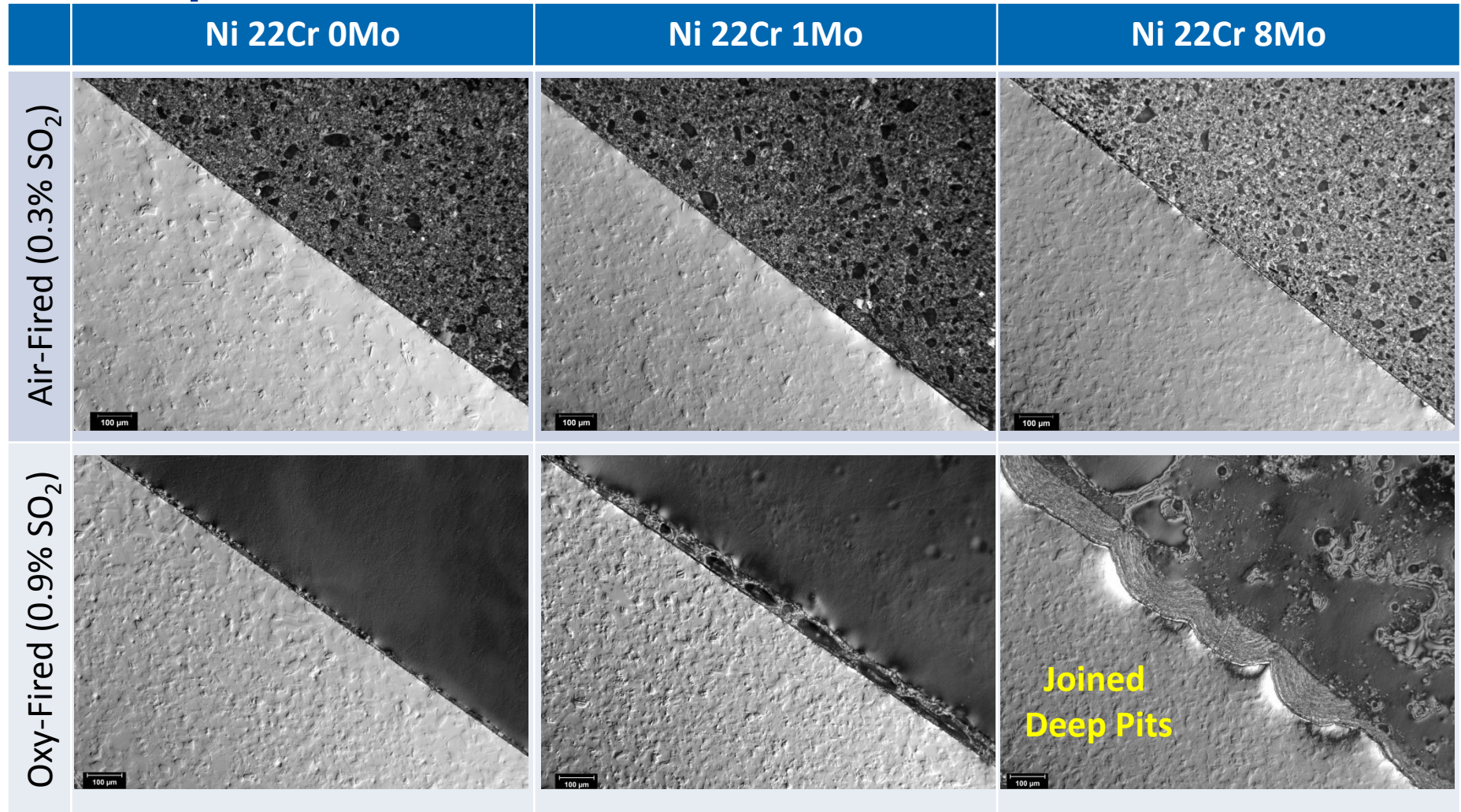
24 hr Exposure at 700°C with an 80% alkali iron trisulfate ash



Large effect from 8 Mo and Gas Phase (SO_x, H₂O, CO₂) with an 80% alkali iron trisulfate ash

Effect of Mo

24 hr Exposure at 700°C with a **100%** alkali iron trisulfate ash



Large effect from 8 Mo and Gas Phase (SO_x, H₂O, CO₂) with a 100% alkali iron trisulfate ash

Summary of New FY14 Oxy-Combustion Fireside Corrosion Research

Aims

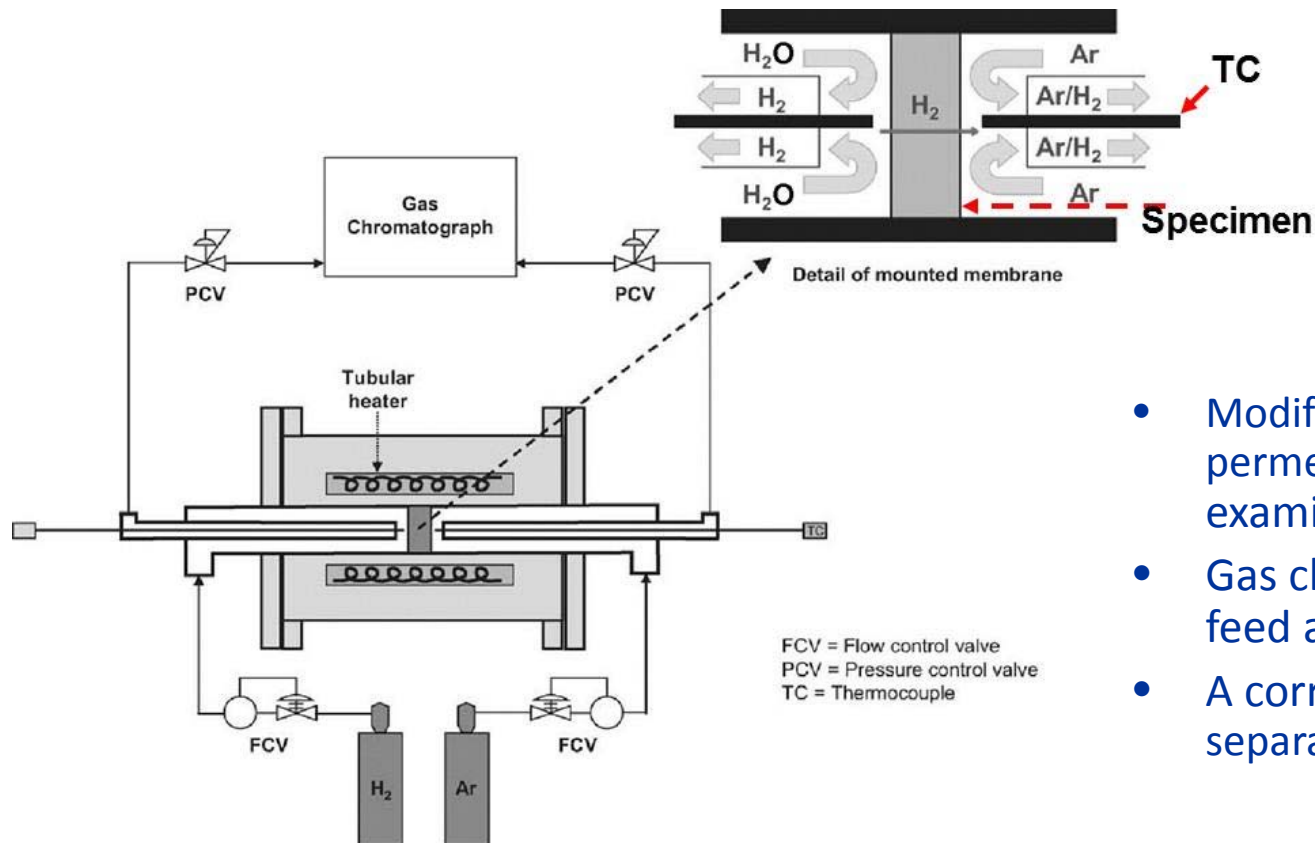
- Temperature effects
- Mo effects with Ni22CrXMo Alloys
- Compare NETL's CPJ7B to T92
- Sulfate flux

Progress

- Fluxing of Fe_3O_4 found for T92 in ash
- Early corrosion initiation with 8Mo in Ni22CrXMo alloys with high sulfate ash levels when combined with high SO_x gases

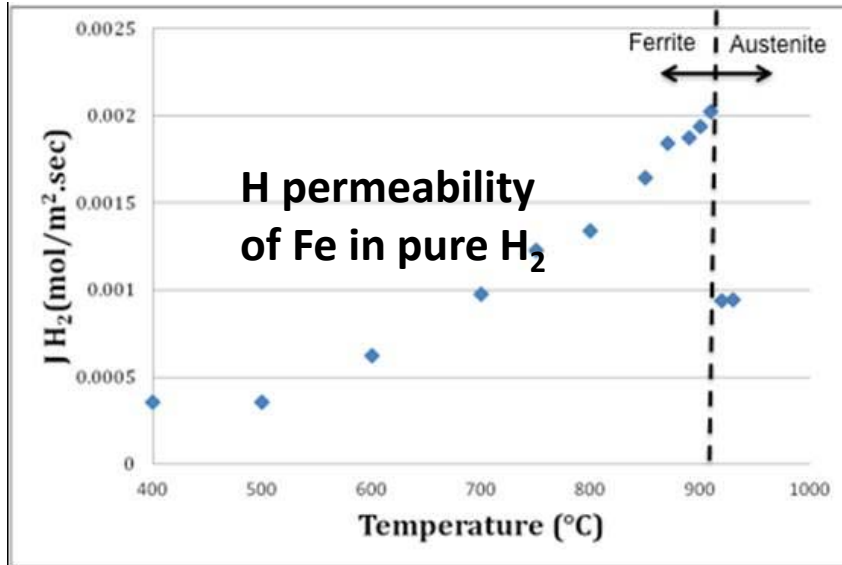
Hydrogen Tracking During Oxidation

- SH/RH boiler corrosion occurs in a mixed oxidant atmosphere (O_2 , CO_2 , H_2O , SO_2)
- Oxyfuel combustion changes the amounts and ratios of oxidants
- This research examines, in a more fundamental nature, the influence of individual oxidants in mixed oxidant gases, and the transport path of hydrogen when it is a product of water oxidation



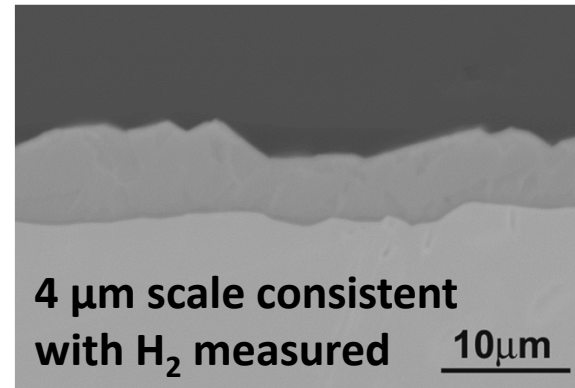
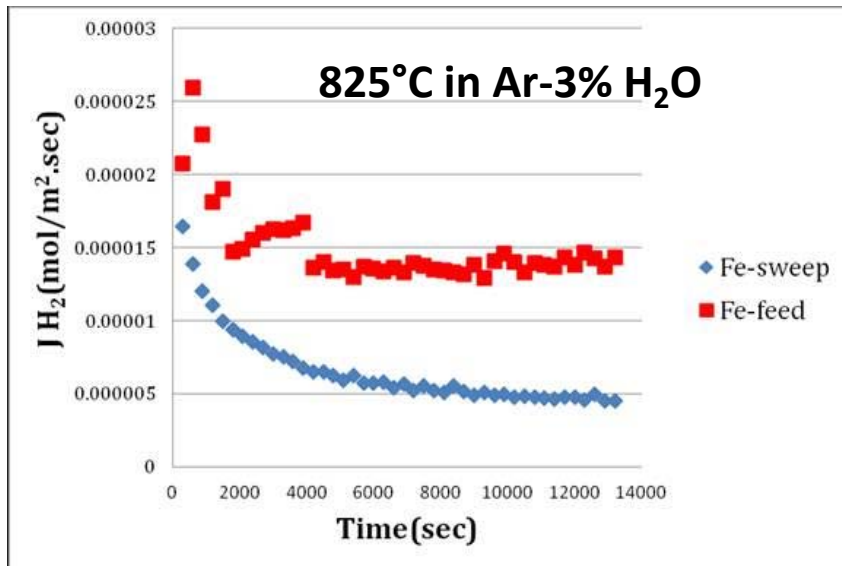
- Modification of a hydrogen permeability apparatus to examine corrosion
- Gas chromatography (GC) of feed and sweep gases
- A corrosion sample foil separates the two gas streams

Results for Fe in Ar-3%H₂O

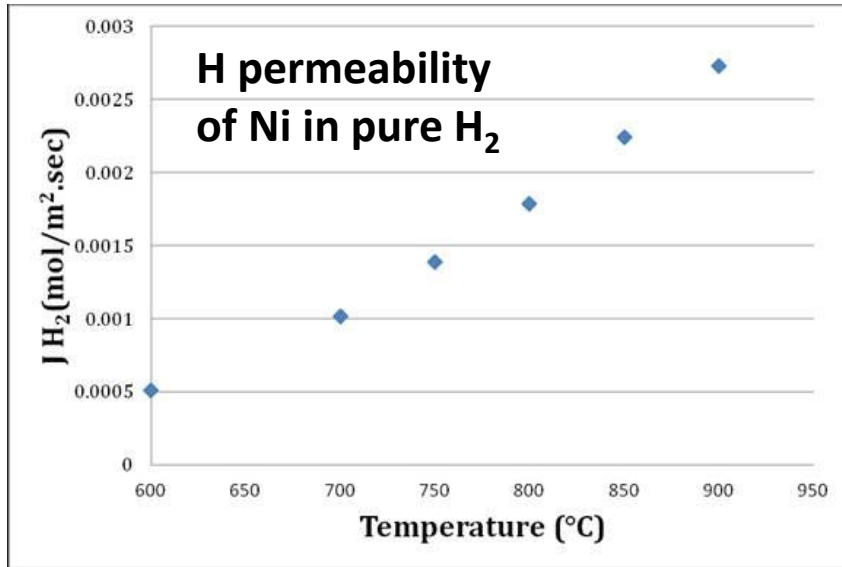


After initial rapid scale growth at 825°C:

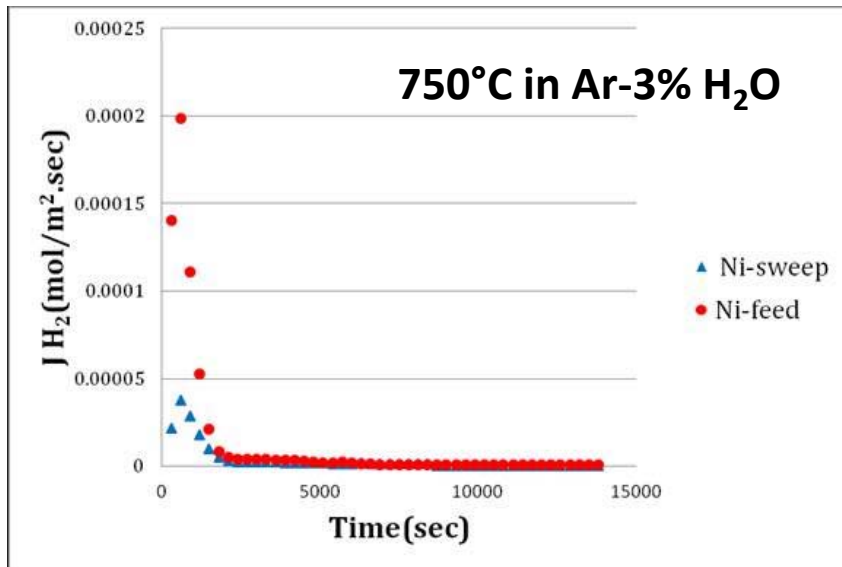
- ~25% of H₂ is injected into and through the metal
- ~75% of H₂ is desorbed back into the feed gas
- Tomlinson and Cory (1989) found the fraction of injected H decreased with increased T
- Short term exposures of Fe at these temperatures in H₂O have linear kinetics and are surface reaction controlled (Turkdogan 1965).
- Estimated fugacities at the Fe/FeO interface using Sievert's law and H permeability data (825°C):
 - H₂ 1 × 10⁻⁵ atm
 - O₂ 4 × 10⁻¹⁹ atm
 - H₂O 5 × 10⁻⁶ atm



Results for Ni in Ar-3%H₂O



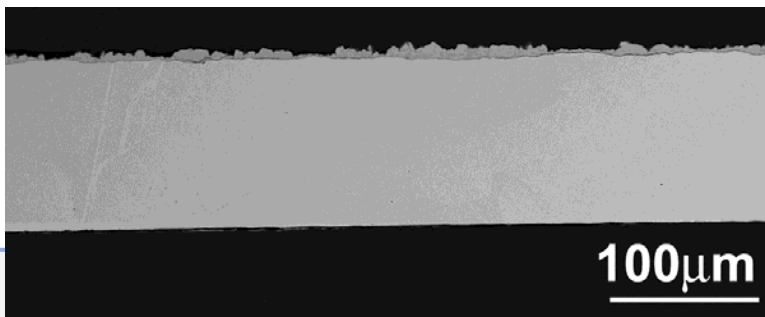
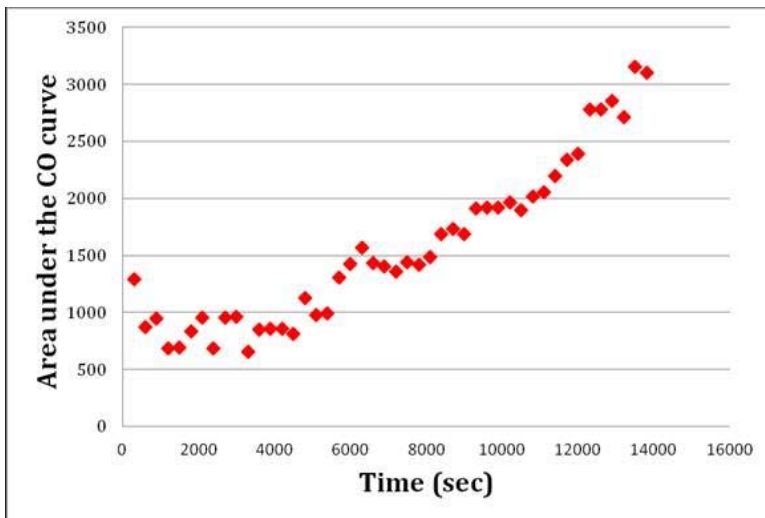
- After initially high fluxes, the feed and sweep H₂ levels become quite low
- Estimated fugacities at the Ni/NiO interface using Sievert's law and H permeability data:
 - H₂ 7×10^{-8} atm
 - O₂ 8×10^{-16} atm
 - H₂O 1×10^{-5} atm



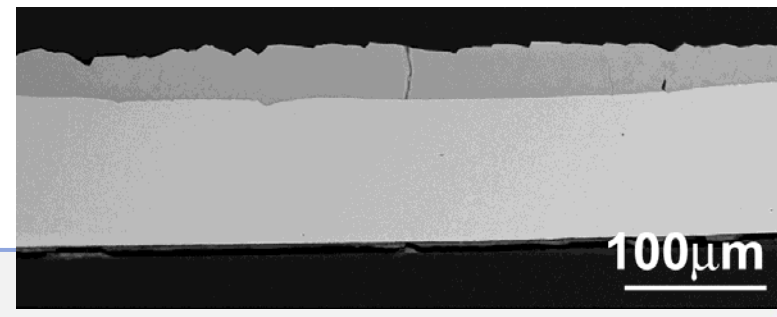
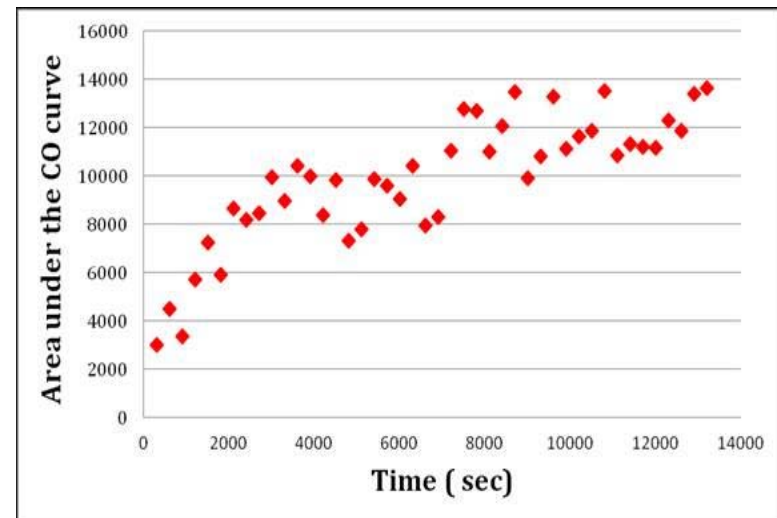
Results for Fe at 750°C in Ar-CO₂-H₂O

- Unlike in Ar-H₂O, these rates continue to increase with time
- Much more oxidation in CO₂ with H₂O than without H₂O
- Sweep and feed gases also contain H₂
- In these short exposures, both H₂O and CO₂ are adsorbing and contributing to the surface reactions, which control the rate of scale growth.

CO Flux in at 750°C in Ar-10%CO₂



CO Flux in at 750°C in Ar-10%CO₂-3%H₂O



Summary of Hydrogen Tracking During Oxidation

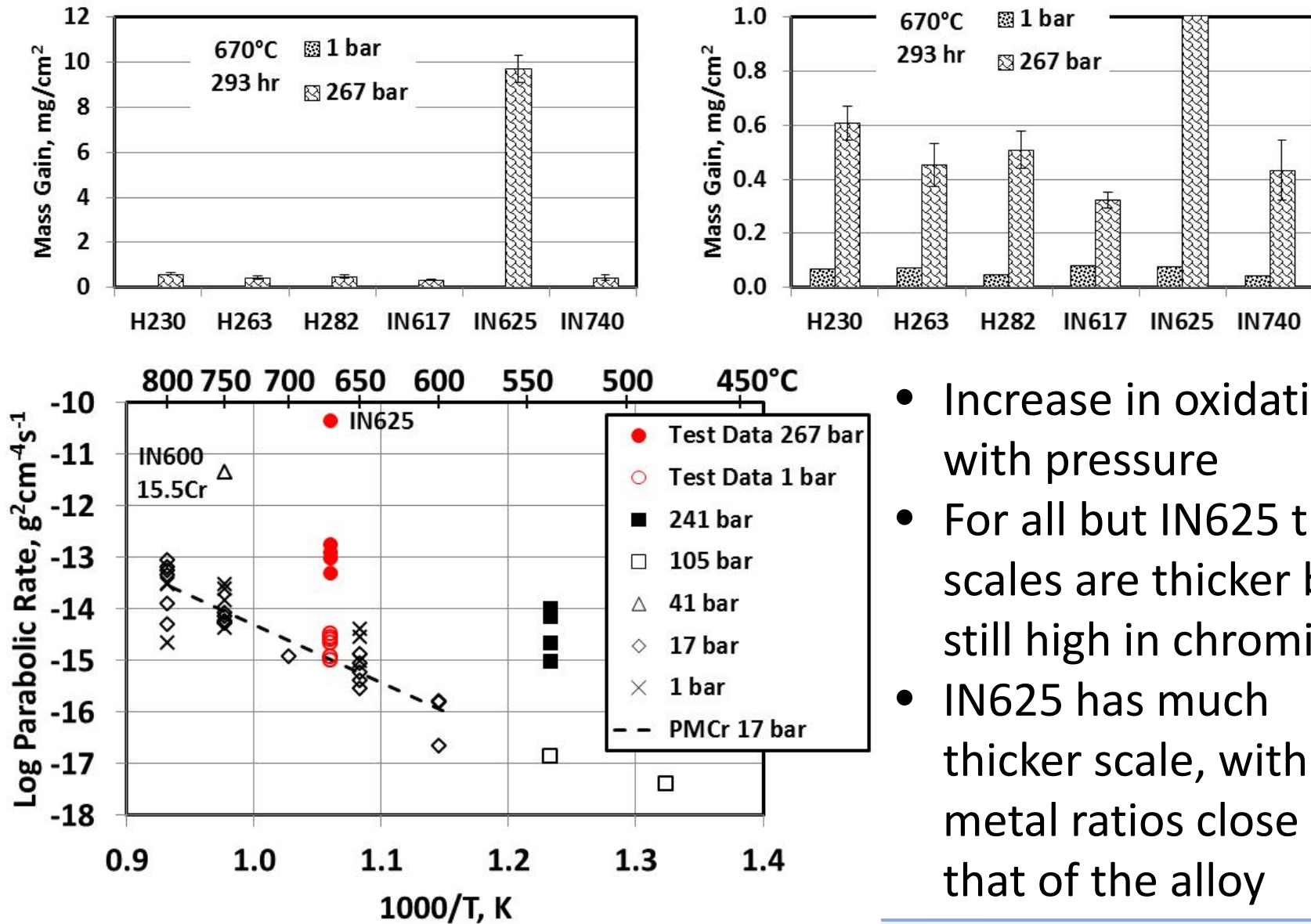
Oxidation in Ar-H₂O

- For Fe, significant hydrogen permeates through.
- Of the H₂ generated, 25% permeated through the foil.
- For Ni, the hydrogen flux drops to very low levels as NiO forms on the surface.
- Activities of H₂, O₂, and H₂O were able to be calculated at the metal-scale interface.

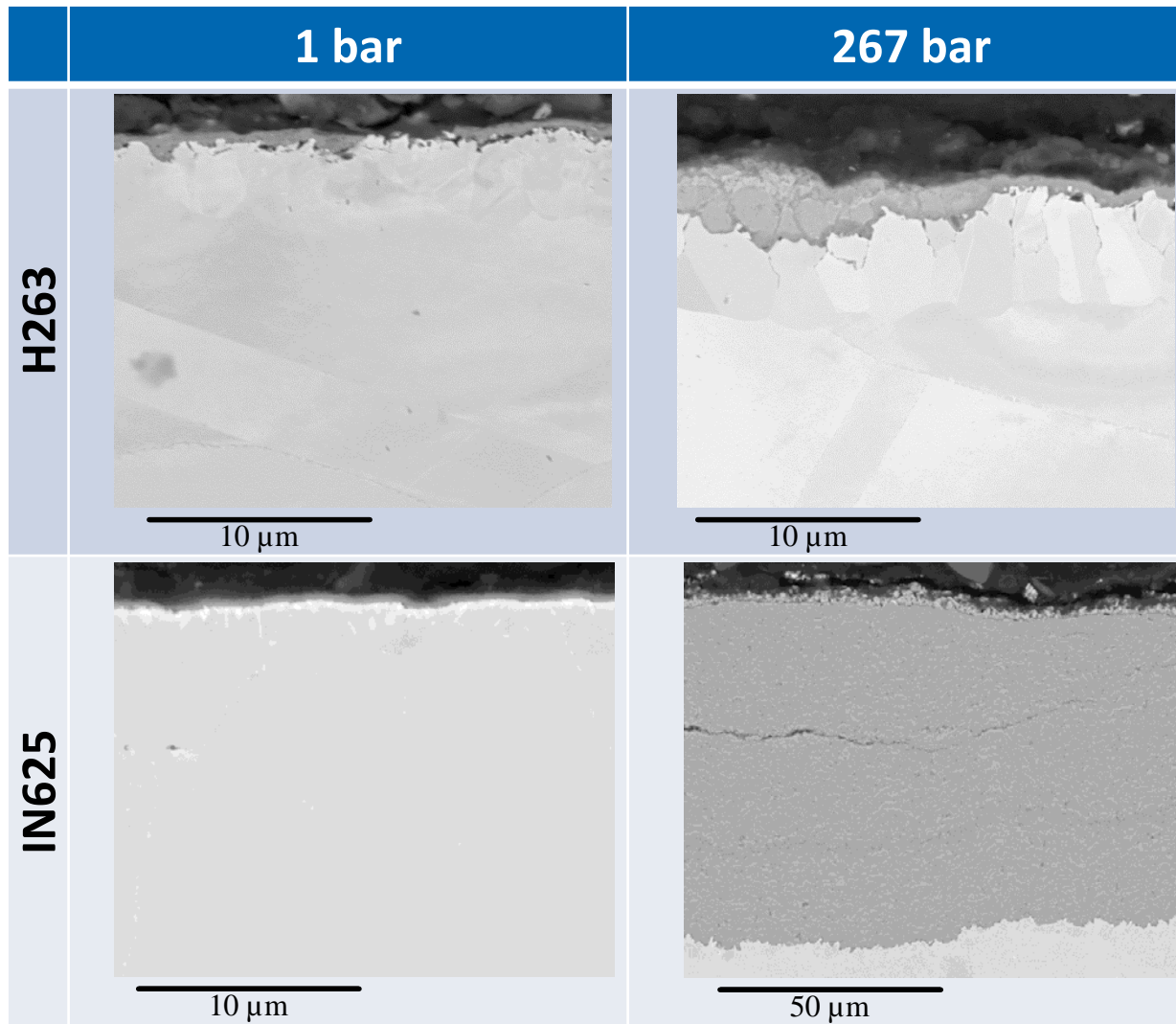
Oxidation in Ar-CO₂ and Ar-CO₂-H₂O

- Oxidation was accelerated in the presence of both CO₂ and H₂O.
- In Ar-CO₂-H₂O, both CO and H₂ were observed in the feed gas.
- Both H₂O and CO₂ absorb and contribute to the surface reactions, which control scale growth.

Update on Steam Oxidation at High Pressure



- Increase in oxidation with pressure
- For all but IN625 the scales are thicker but still high in chromia
- IN625 has much thicker scale, with metal ratios close to that of the alloy



Selected for TEM Analysis

- Why does higher pressure increase corrosion?
- What is going on with IN625?
- IN625 has high Mo precipitates near the surface, not found for other alloys

Compositions of alloys (wt%) measured by x-ray fluorescence											
Alloy	Fe	Cr	Ni	Co	Mo	Si	Ti	Al	Mn	Nb	Cu
H263		20.0	Bal	20.1	5.7	0.3	2.1	0.3	0.5	0.1	
IN625	4.4	21.4	Bal	0.1	8.4	0.3	0.3	0.2	0.1	3.3	0.3